



Published in final edited form as:

*Clin Pharmacol Ther.* 2013 July ; 94(1): 19–23. doi:10.1038/clpt.2013.73.

## SLC classification: an update

Avner Schlessinger<sup>1,2,\*</sup>, Sook Wah Yee<sup>3,4</sup>, Andrej Sali<sup>3,4,5</sup>, and Kathleen M. Giacomini<sup>3,4,6,\*</sup>

<sup>1</sup>Department of Pharmacology and Systems Therapeutics, Mount Sinai School of Medicine, New York, NY 10029.

<sup>2</sup>Tisch Cancer Institute, Mount Sinai School of Medicine, New York, NY 10029.

<sup>3</sup>Department of Bioengineering and Therapeutic Sciences, University of California, San Francisco, CA 94158.

<sup>4</sup>California Institute for Quantitative Biosciences, University of California, San Francisco, CA 94158.

<sup>5</sup>Department of Pharmaceutical Chemistry, University of California, San Francisco, CA 94158.

<sup>6</sup>Institute for Human Genetics, University of California, San Francisco, CA 94158.

## Sequence-based similarity networks

A sequence similarity network is made up of links corresponding to pairwise relationships that score better than a defined cutoff<sup>1,2</sup> (Fig. 1). Pairwise sequence alignment scores, including percent sequence identity and Expectation Value (E-Value), were computed using SALIGN<sup>3</sup>. The E-value of a match is the number of sequences in the queried database that are expected to match by chance the query sequence at least as well as the assessed match; smaller values indicate more statistically significant alignments<sup>3</sup>. The E-value cutoffs for the final similarity networks were selected manually, similarly to our previous analysis<sup>1,2</sup>. Because of the small database that was used for the analysis (i.e., 386 sequences), E-value cutoffs that typically do not represent meaningful relationship among sequences when using large databases (e.g., E-value of 1) were also considered. Finally, the graphs representing the similarity networks were visualized using Cytoscape 2.8.1<sup>4</sup>. We used the yFiles organic layout algorithm, which maintains all the connections between the nodes to illustrate relationships. Groups of nodes that are inter-connected usually cluster together in the network.

## Sequence similarity between human SLC sequences and PDB structures

For each transporter structure, we retrieved the amino acid sequence from the UniProt database<sup>5</sup>. We then ran the alignment server HHpred<sup>6</sup> against the human proteome, using the default parameters. Finally, we selected the alignment between the query sequence of known structure and the human transporter protein with the highest sequence identity, and also retrieved the E-value for the alignment (Table 1 and Supplementary Table 1).

\*Corresponding author: Avner Schlessinger, avner.schlessinger@mssm.edu Kathleen M. Giacomini, kathy.giacomini@ucsf.edu.

## Atomic structures of homologs of drug ADME SLC transporters

The structures described in Table 1 are of the amino acid antiporter AdiC from *Escherichia coli*<sup>7</sup>, the homolog of the apical sodium-dependent bile acid transporter from *Neisseria meningitidis* (ASBT<sub>NM</sub>)<sup>8</sup>, the peptide transporter from *Shewanella oneidensis* (PepT<sub>SO</sub>)<sup>9</sup>, the high-affinity phosphate importer PiPT from *Piriformospora indica*<sup>10</sup>, the concentrative nucleoside transporter from *Vibrio cholera* (vcCNT)<sup>11</sup>, and the multidrug and toxic compound extrusion transporter NorM from *Vibrio cholera*<sup>12</sup>.

## Supplementary Material

Refer to Web version on PubMed Central for supplementary material.

## REFERENCES

- Atkinson HJ, Morris JH, Ferrin TE, Babbitt PC. Using sequence similarity networks for visualization of relationships across diverse protein superfamilies. *PLoS ONE*. 2009; 4:e4345. [PubMed: 19190775]
- Schlessinger A, et al. Comparison of human solute carriers. *Protein science : a publication of the Protein Society*. 2010; 19:412–428. [PubMed: 20052679]
- Madhusudhan MS, Webb BM, Marti-Renom MA, Eswar N, Sali A. Alignment of multiple protein structures based on sequence and structure features. *Protein Eng Des Sel*. 2009; 22:569–574. [PubMed: 19587024]
- Shannon P, et al. Cytoscape: a software environment for integrated models of biomolecular interaction networks. *Genome Res*. 2003; 13:2498–2504. [PubMed: 14597658]
- The Universal Protein Resource (UniProt) in 2010. *Nucleic acids research*. 2010; 38:D142–D148. [PubMed: 19843607]
- Soding J, Biegert A, Lupas AN. The HHpred interactive server for protein homology detection and structure prediction. *Nucleic acids research*. 2005; 33:W244–W248. [PubMed: 15980461]
- Gao X, et al. Mechanism of substrate recognition and transport by an amino acid antiporter. *Nature*. 2010; 463:828–832. [PubMed: 20090677]
- Hu NJ, Iwata S, Cameron AD, Drew D. Crystal structure of a bacterial homologue of the bile acid sodium symporter ASBT. *Nature*. 2011; 478:408–411. [PubMed: 21976025]
- Newstead S, et al. Crystal structure of a prokaryotic homologue of the mammalian oligopeptide-proton symporters, PepT1 and PepT2. *The EMBO journal*. 2011; 30:417–426. [PubMed: 21131908]
- Pedersen BP, Kumar H, Waight AB, Risenmay AJ, Roe-Zurz Z, Chau BH, Schlessinger A, Bonomi M, Harries W, Sali A, Johri AK, Stroud RM. Crystal structure of a eukaryotic phosphate transporter. *Nature*. 2013
- Johnson ZL, Cheong CG, Lee SY. Crystal structure of a concentrative nucleoside transporter from *Vibrio cholerae* at 2.4 Å. *Nature*. 2012; 483:489–493. [PubMed: 22407322]
- He X, et al. Structure of a cation-bound multidrug and toxic compound extrusion transporter. *Nature*. 2010; 467:991–994. [PubMed: 20861838]
- Sonnhammer EL, von Heijne G, Krogh A. A hidden Markov model for predicting transmembrane helices in protein sequences. *Proc Int Conf Intell Syst Mol Biol*. 1998; 6:175–182. [PubMed: 9783223]
- Nugent T, Jones DT. Transmembrane protein topology prediction using support vector machines. *BMC bioinformatics*. 2009; 10:159. [PubMed: 19470175]
- Bernsel A, Viklund H, Hennerdal A, Elofsson A. TOPCONS: consensus prediction of membrane protein topology. *Nucleic acids research*. 2009; 37:W465–W468. [PubMed: 19429891]
- Yernool D, Boudker O, Jin Y, Gouaux E. Structure of a glutamate transporter homologue from *Pyrococcus horikoshii*. *Nature*. 2004; 431:811–818. [PubMed: 15483603]

17. Sun L, et al. Crystal structure of a bacterial homologue of glucose transporters GLUT1-4. *Nature*. 2012; 490:361–366. [PubMed: 23075985]
18. Faham S, et al. The crystal structure of a sodium galactose transporter reveals mechanistic insights into Na<sup>+</sup>/sugar symport. *Science*. 2008; 321:810–814. [PubMed: 18599740]
19. Yamashita A, Singh SK, Kawate T, Jin Y, Gouaux E. Crystal structure of a bacterial homologue of Na<sup>+</sup>/Cl<sup>-</sup>-dependent neurotransmitter transporters. *Nature*. 2005; 437:215–223. [PubMed: 16041361]
20. Mancusso R, Gregorio GG, Liu Q, Wang DN. Structure and mechanism of a bacterial sodium-dependent dicarboxylate transporter. *Nature*. 2012; 491:622–626. [PubMed: 23086149]
21. Berardi MJ, Shih WM, Harrison SC, Chou JJ. Mitochondrial uncoupling protein 2 structure determined by NMR molecular fragment searching. *Nature*. 2011; 476:109–113. [PubMed: 21785437]
22. Huang Y, Lemieux MJ, Song J, Auer M, Wang DN. Structure and mechanism of the glycerol-3-phosphate transporter from *Escherichia coli*. *Science*. 2003; 301:616–620. [PubMed: 12893936]
23. Hediger MA, et al. The ABCs of solute carriers: physiological, pathological and therapeutic implications of human membrane transport proteinsIntroduction. *Pflugers Arch*. 2004; 447:465–468. [PubMed: 14624363]

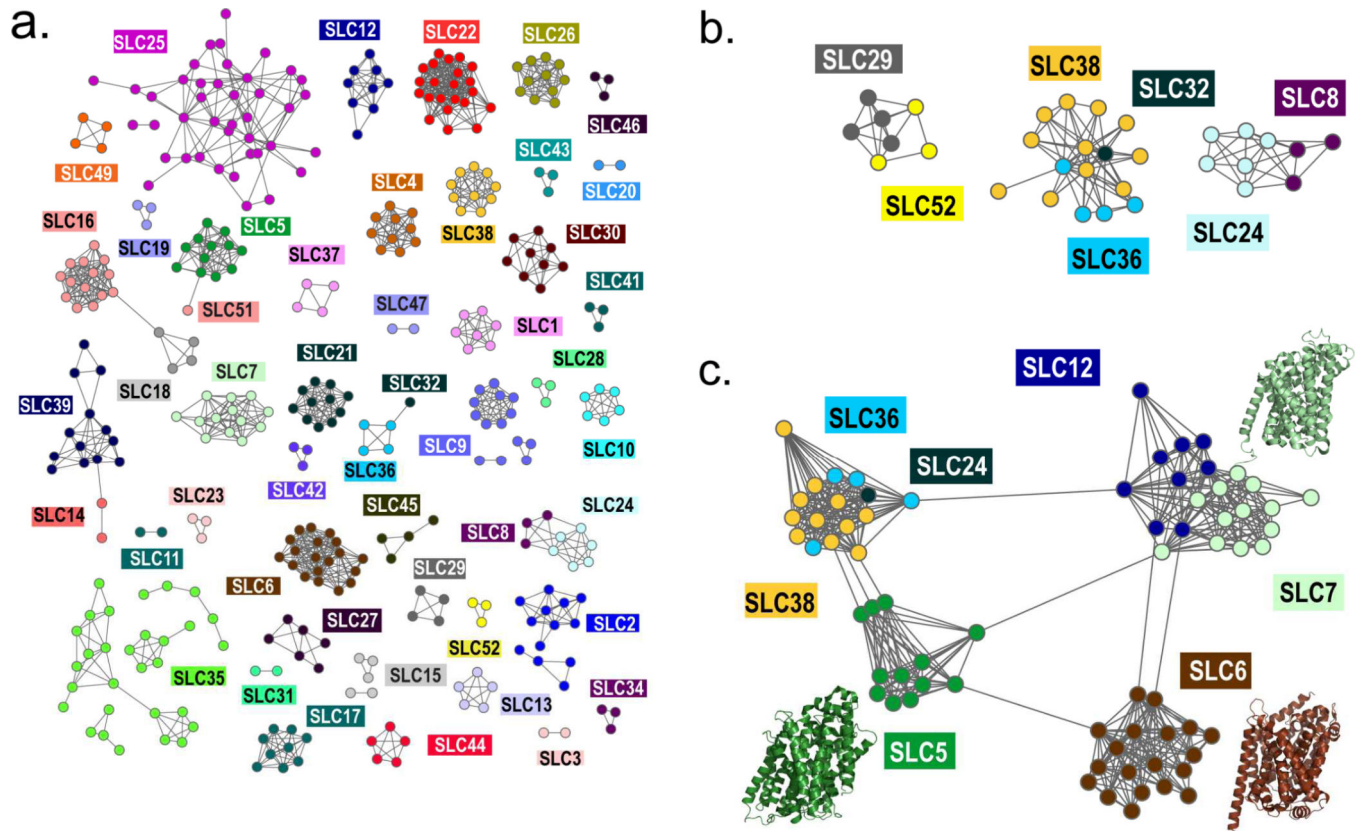
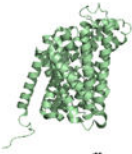
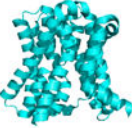



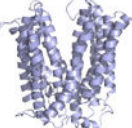


Figure 1.

**Table 1**

Drug ADME SLC families that can be modeled based on atomic resolution structures from other organisms.

Family <sup>a</sup>	Function <sup>b</sup>	Template Structure <sup>c</sup>	Percent Sequence Identity <sup>d</sup>	Representative Drug Substrates <sup>e</sup>
SLC7 (14)	Cationic amino acid transporter/glycoprotein-associated family	 AdIC <sup>#</sup>	21 ( $1.4 \times 10^{-47}$ )	Melphalan, gabapentin, levodopa, baclofen
SLC10 (7)	Na <sup>+</sup> bile salt co-transporters	 ASBT <sub>NM</sub>	26 ( $1.8 \times 10^{-42}$ )	Rosuvastatin, atorvastatin, fluvastatin
SLC15 (4)	Proton oligopeptide co-transporters	 PepT <sub>so</sub> <sup>*</sup>	34 ( $2.2 \times 10^{-28}$ )	Valacyclovir, cephalexin, cefadroxil, enalapril, captopril
SLC22 (26)	Organic cation/anion/zwitterion transporters	 PiPT <sup>*</sup>	20 ( $4.9 \times 10^{-34}$ )	Metformin, acyclovir, methotrexate, olmesartan, ipratropium, oxaliplatin, cimetidine
SLC28 (3)	Na <sup>+</sup> -coupled nucleoside transporters	 vcCNT	40 ( $6.4 \times 10^{-130}$ )	Fludarabine, gemcitabine, cytarabine
SLC47 (2)	Multidrug and toxin extrusion (MATE) transporters	 NorM	23 ( $4.8 \times 10^{-51}$ )	Metformin, trospium, fexofenadine

<sup>a</sup> Family marks the human SLC family, as annotated by the Bioparadigms database<sup>2</sup>. The number of human protein sequences in the family is provided in parenthesis.

<sup>b</sup> *Function* gives the function of the human family, as described in the Bioparadigms database

<sup>c</sup> *Template Structure* describes the most related atomic structure to the family. Structures with the MFS and NSS folds are marked with '\*' and '#', respectively. Detailed description of the structures, including the full name of the proteins and the corresponding references are described in the Supplementary Material.

<sup>d</sup> *Percent Sequence Identity* provides the percent sequence identity of the best scoring hit from each family; E-value is given in parenthesis (Supplementary Material)

<sup>e</sup> *Representative Drug Substrates* gives examples of key prescription drugs that are substrates of the transporter.